

# Variational quantum metrology for multiparameter estimation under dephasing noise

Trung Kien Le,<sup>1</sup> Hung Q. Nguyen,<sup>2</sup> and Le Bin Ho<sup>3,4,\*</sup>

<sup>1</sup>*Department of Physics, University of California, Santa Barbara, USA*

<sup>2</sup>*Nano and Energy Center, VNU University of Science, Vietnam National University, Hanoi*

<sup>3</sup>*Frontier Research Institute for Interdisciplinary Sciences, Tohoku University, Sendai 980-8578, Japan*

<sup>4</sup>*Department of Applied Physics, Graduate School of Engineering, Tohoku University, Sendai 980-8579, Japan*

We present a hybrid quantum-classical variational scheme to enhance precision in quantum metrology. In the scheme, both the initial state and the measurement basis in the quantum part are parameterized and optimized via the classical part. It enables the maximization of information gained about the measured quantity. We discuss specific applications to 3D magnetic field sensing under several dephasing noise modes. Indeed, we demonstrate its ability to simultaneously estimate all parameters and surpass the standard quantum limit, making it a powerful tool for metrological applications.

## I. INTRODUCTION

Quantum metrology is an estimation process that utilizes unique quantum phenomena such as entanglement and squeezing to improve the precision of estimation beyond classical limits [6, 15, 44]. Recent development in quantum computing leads to numerous optimal algorithms for enhancing precision in single-parameter estimation, such as adaptive measurements [3, 9, 13, 54], quantum error correction [25, 56], and optimal quantum control [36, 50, 51]. So far, a variational algorithm has been demonstrated by combining the advantages of both quantum and classical systems for quantum-enhanced metrology [21, 27, 29, 51]. A similar protocol for spin systems was also introduced [22, 55]. More recently, such a variational toolbox for multiparameter estimation was proposed [32], which is a generalization from the previous work mentioned above [29].

While using variational schemes is promising, their potential significance in multiparameter quantum metrology has yet to fully understand, even in principle. Furthermore, determining the optimal quantum resources and measurement strategy to extract maximum information about all parameters is challenging due to the trade-offs in estimating incompatible observables [39, 57]. Therefore, a suitable method for precisely estimating of multiparameter remains a thriving area of research in quantum metrology.

In this work, we propose a variational scheme to enhance the precision of multiparameter estimation in the presence of dephasing noise. The basic idea is to use a quantum computer to prepare a trial state (an ansatz) that depends on a set of trainable variables. The state is subjected to a series of control operations, representing unknown multiparameter and noise, and then is measured through observables determined by other trainable variables. The measurement results are used to update the trainable variables and optimize the estimation of the unknown multiparameter.

Optimizing both the initial quantum state and the measure-

ment operators allows us to identify suitable conditions for the quantum probe to increase sensitivity and achieve the ultimate quantum limit for all parameters. In numerical simulations, we estimate a 3D magnetic field under a dephasing noise model and find that sensitivity for all parameters can simultaneously reach the ultimate quantum bound. We also examine a time-dependent Ornstein-Uhlenbeck model [45] and observe results surpassing the standard quantum limit by increasing the probe's number of particles. This approach holds promise for a wide range of metrological applications, including external field sensing, precision spectroscopy, gravitational wave detection, and others.

## II. RESULTS

### A. Variational quantum metrology

The goal of multiparameter estimation is to evaluate a set of unknown parameters  $\phi = (\phi_1, \phi_2, \dots, \phi_M)^\top$ , which are imprinted onto a quantum probe via a unitary evolution  $U(\phi) = \exp(-it\mathbf{H}\phi) = \exp(-it\sum_{k=1}^M H_k \phi_k)$ , where  $\mathbf{H} = (H_1, H_2, \dots, H_M)$  are non-commuting Hermitian Hamiltonians. The precision of estimated parameters  $\check{\phi}$  is evaluated using a mean square error matrix (MSEM)  $V = \sum_m p(m|\phi) [\check{\phi}(m) - \phi] [\check{\phi}(m) - \phi]^\top$ , where  $p(m|\phi) = \text{Tr}[\rho(\phi)E_m]$  is the probability for obtaining an outcome  $m$  when measuring the final state  $\rho(\phi)$  by an element  $E_m$  in a positive, operator-value measure (POVM). The MSEM obeys the Cramér-Rao bounds (CRBs) [17, 19]

$$\text{Tr}[WV] \geq C_F \geq C_H \geq C_Q, \quad (1)$$

where  $W$  is a scalar weight matrix,  $C_F = \text{Tr}[WF^{-1}]$  is a classical bound, where  $F$  is the classical Fisher information matrix (CFIM) with elements  $F_{ij} = \sum_m \frac{1}{p(m|\phi)} [\partial_{\phi_i} p(m|\phi)] [\partial_{\phi_j} p(m|\phi)]$  [37]. The Holevo bound  $C_H$  is given via semidefinite programming, i.e.,  $C_H = \min_{\{X_i\}} (\text{Tr}[W\text{Re}Z + \|\sqrt{W}\text{Im}Z\sqrt{W}\|_1])$  [16, 19], where  $Z$  is a positive semidefinite matrix with elements  $Z_{ij} = \text{Tr}[X_i X_j \rho(\phi)]$ , and a set of matrices  $\{X_i\}$  satisfies  $\text{Tr}[X_i \partial_{\phi_j} \rho(\phi)] = \delta_{ij}$ .

\*Electronic address: binho@riec.tohoku.ac.jp

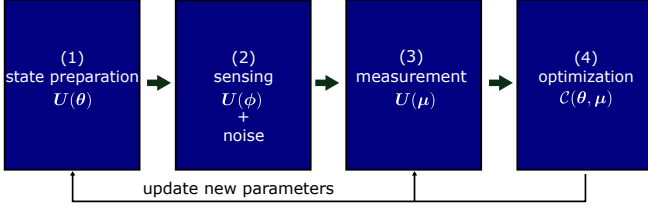


FIG. 1: **Variational quantum metrology.** (1) use quantum circuit  $U(\theta)$  to prepare a variational state; (2) encode multiparameter  $\phi$  and noise using  $U(\phi)$  and noise channels; (3) use circuit  $U(\mu)$  to create a variational POVM for measurement; (4) send measurement results to a classical computer to optimize cost function  $\mathcal{C}(\theta, \mu)$  using a gradient-based optimizer. Update new training variables and repeat the scheme until it converges.

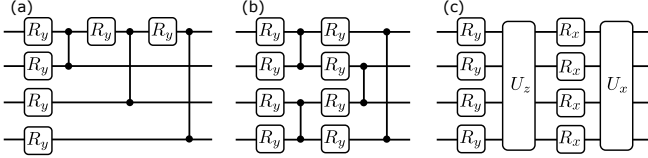


FIG. 2: **Ansatzes for preparation state and POVM.** (a) star topology entangled ansatz. (b) ring topology entangled ansatz. (c) squeezing ansatz. In the circuits,  $R_{x(y)}$ :  $x(y)$ -rotation gate,  $U_{x(z)}$ : global Mølmer-Sørensen gate,  $\bullet\bullet$ : controlled-Z gate.

Finally,  $C_Q = \text{Tr}[WQ^{-1}]$  is a quantum bound where  $Q_{ij} = \text{Re}[\text{Tr}[\rho(\phi)L_iL_j]]$  is the real symmetric quantum Fisher information matrix (QFIM) that defined through the symmetric logarithmic derivative (SLD)  $2\partial_{\phi_j}\rho(\phi) = \{L_j, \rho(\phi)\}$  [37].

Although optimal estimators can achieve  $C_F$  [23] and asymptotic achievement of  $C_H$  is possible [1, 12, 42, 49, 52], it is impossible to attain the quantum bound for multiparameter estimation [16]. In some instances,  $C_H = C_Q$  if a weak commutativity condition  $\text{Im}(\text{Tr}[L_jL_i\rho(\phi)]) = 0$  is met [10, 16]. The same condition also applies to attain  $C_F = C_Q$  [31]. However, this condition alone is insufficient to achieve the quantum bound practically; a proper POVM is also required.

This paper presents a variational quantum metrology (VQM) scheme following Meyer et al. toolbox [32] as sketched in Fig. 1 to optimize both the preparation state and POVM. A quantum circuit  $U(\theta)$  is used to generate a variational preparation state with trainable variables  $\theta$ . Similar quantum circuit with variables  $\mu$  is used to generate a variational POVM  $E(\mu) = \{E_m(\mu) = U^\dagger(\mu)E_mU(\mu) > 0 | \sum_m E_m(\mu) = I\}$ . Using classical computers, a cost function  $\mathcal{C}(\theta, \mu)$  can be optimized to generate new variables for quantum circuits, resulting in enhanced information extraction. The scheme is repeated until it converges.

To investigate the ultimate quantum bound, we define the cost function by a relative difference [1]

$$\mathcal{C}(\theta, \mu) = 1 - \frac{C_Q}{C_F}, \quad (2)$$

which is positive semidefinite according to Eq. (1). The variables are trained by solving the optimization task  $\arg \min \mathcal{C}(\theta, \mu)$ . As the value of  $\mathcal{C}(\theta, \mu)$  approaches zero, we  $\{\theta, \mu\}$

reach the ultimate quantum bound where  $\text{Tr}[WV] = C_F = C_Q$ . A vital feature of the VQM is using variational quantum circuits, which allow for optimizing the circuits to extract the maximum information about the estimated parameters.

## B. Ansatzes

We propose three variational circuits: a star topology ansatz, a ring topology ansatz, and a squeezing ansatz. The first two ansatzes are inspired by quantum graph states, which are useful resources for quantum metrology [41, 48]. A conventional graph state is formed by a collection of vertices  $V$  and edges  $D$  as  $G(V, D) = \prod_{i,j \in D} CZ^{ij}|+\rangle^V$ , where  $CZ^{ij}$  represents the controlled-Z gate connecting the  $i$  and  $j$  qubits, and  $|+\rangle$  is an element in the basis of Pauli  $\sigma_x$ . The proposed ansatzes here incorporate  $y$ -rotation gates ( $R_y(\theta) = e^{-i\theta\sigma_y/2}$ ) at every vertex prior to CZ gates (see Fig. 2a,b). The squeezing ansatz in Fig. 2c is inspired by squeezing states, which is another useful resource for quantum metrology [7, 14, 30]. It has  $x(y)$ -rotation gates and global Mølmer-Sørensen gates  $U_{x(z)}$ , where  $U_{x(z)} = \exp(-i \sum_{j=1}^N \sum_{k=j+1}^N \sigma_{x(z)} \otimes \sigma_{x(z)} \frac{\chi_{jk}}{2})$  for an  $N$ -qubit circuit [34]. The trainable variables for one layer are  $2N - 2$ ,  $2N$ , and  $N(N + 1)$  for the star, ring, and squeezing ansatz, respectively. Hereafter, we use these ansatzes for generating variational preparation states and variational POVM in the VQM scheme.

## C. Multiparameter estimation under dephasing noise

After preparing a variational state  $\rho(\theta) = U(\theta)\rho_0U(\theta)$ , we use it to estimate a 3D magnetic field under dephasing noise. The field is imprinted onto every single qubit via the Hamiltonian  $H = \sum_{i \in \{x,y,z\}} \phi_i \sigma_i$ , where  $\phi = (\phi_x, \phi_y, \phi_z)$ , and  $\sigma_i$  is a Pauli matrix. Under dephasing noise, the variational state  $\rho(\theta)$  evolves to [28]

$$\mathcal{E}_t(\rho) = \left[ \prod_{k=1}^N e^{\gamma t \mathcal{L}^{(k)}} \right] e^{-it\mathcal{H}} \rho, \quad (3)$$

where we omitted  $\theta$  in  $\rho(\theta)$  for short. The superoperator  $\mathcal{H}$  generates a unitary dynamic  $\mathcal{H}\rho = [H, \rho]$ , and  $\mathcal{L}^{(k)}$  is a non-unitary dephasing superoperator with  $\gamma$  is the decay rate. In terms of Kraus operators, the dephasing superoperator gives

$$e^{\gamma t \mathcal{L}^{(k)}} \rho = K_1^{(k)} \rho [K_1^{(k)}]^\dagger + K_2^{(k)} \rho [K_2^{(k)}]^\dagger, \quad (4)$$

where  $K_1 = \begin{pmatrix} \sqrt{1-\lambda} & 0 \\ 0 & 1 \end{pmatrix}$  and  $K_2 = \begin{pmatrix} \sqrt{\lambda} & 0 \\ 0 & 0 \end{pmatrix}$  are Kraus operators, and  $\lambda = 1 - e^{-\gamma t}$  is the dephasing probability. Finally, the state is measured in the variational POVM  $E(\mu)$  and yields the probability  $p(m) = \text{Tr}[\mathcal{E}_t(\rho)E_m(\mu)]$ . Note that  $p$  also depends on  $\theta$ ,  $\phi$ , and  $\mu$ .

It is important to attain the ultimate quantum bound, i.e.,  $C_F = C_Q$ . We thus compare numerical results for the cost function,  $C_F$ , and  $C_Q$  as shown in the top panels of Fig. 3. The cost function is plotted after stopping the training by

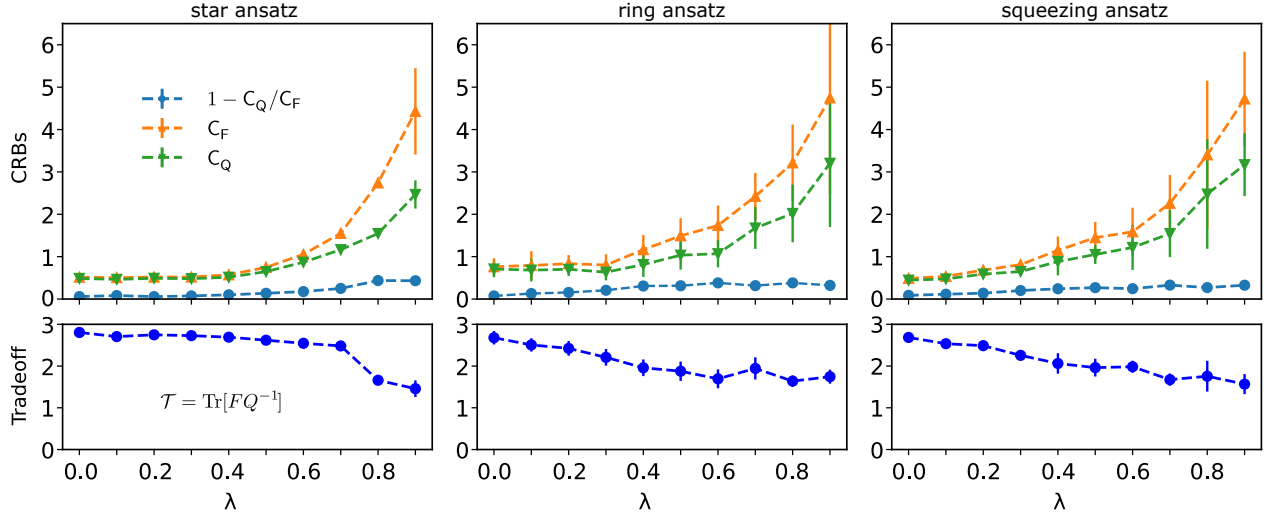


FIG. 3: **Variational quantum metrology under dephasing noise.** (Top): plot of the optimal cost function  $\mathcal{C}(\theta, \mu)$ , classical bound  $C_F$ , and quantum bound  $C_Q$  as functions of dephasing probability. From left to right: star, ring, and squeezing ansatz. (Bottom): plot of corresponding tradeoff  $\mathcal{T}$ . Numerical results are calculated at  $N = 3$ , the optimal number of layers in Fig. 7, and the results are averaged after 10 samples.

EarlyStopping callback [24]. The numerical results are presented at  $N = 3$ , and the number of layers is chosen from their optimal values as shown in the Method and Fig. 7. We find that for small noises,  $C_F$  reaches the ultimate quantum bound, which is consistent with earlier numerical findings [12]. We also compare the performance of the star ansatz to that of the ring and squeezing ansatzes. It saturates the ultimate quantum limit for dephasing probabilities  $\lambda < 0.5$ , whereas the ring and squeezing ansatzes only reach the limit for  $\lambda < 0.2$ . The star graph exhibits a central vertex connected to the remaining  $N - 1$  surrounding vertices, which facilitates robust quantum metrology, as discussed in [41].

Furthermore, we evaluate the tradeoff between the CFIM and QFIM by introducing a function  $\mathcal{T} = \text{Tr}[FQ^{-1}]$ . For unknown  $M$  parameters, the naive bound is  $\max(\mathcal{T}) = M$ , leading to simultaneous optimization of all parameters. The results are shown in the bottom panels of Fig. 3 and agree well with the CRBs presented in the top panels, wherein  $\mathcal{T} \rightarrow 3$  whenever the quantum bound is reached. So far, we observe that  $\mathcal{T} > M/2$  for all cases, which is better than the theoretical prediction previously [46]. This observation exhibits an advantage of the VQM approach.

#### D. Barren Plateaus

Variational quantum circuits under the influence of noises will exhibit a barren plateau (BP), where the gradient along any direction of the variables' space vanishes exponentially with respect to the noise level [47]. The BP prevents reaching the global optimization of the training space, thereby reducing the efficiency and trainability of the variational quantum circuit.

The deviation of CRBs shown in Fig. 3 may be subject to the BP raised by noise. We examine such dependent and show the results in Fig. 4. We plot  $\text{Var}[\partial_{\theta_1} \mathcal{C}]$  where  $\mathcal{C}$  is defined in Eq. (2) after 200 runs with random initialization of  $\theta$  and

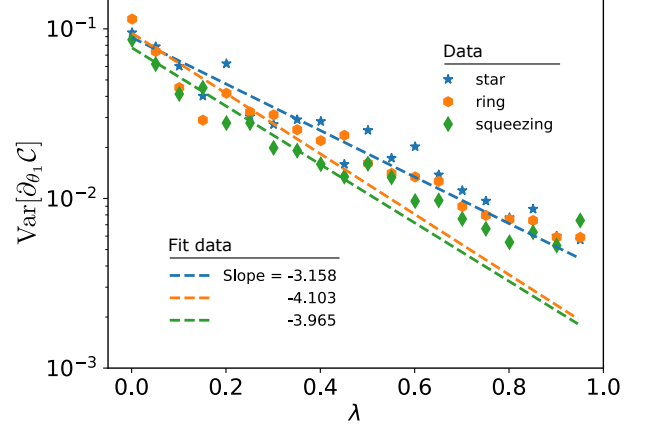


FIG. 4: **Barren plateau.** The variance of gradient  $\text{Var}[\partial_{\theta_1} \mathcal{C}]$  is plotted as a function of the dephasing probability  $\lambda$ . The slope of each fit line indicates the exponential decay of the gradient, which is a sign of the barren plateau effect.

$\mu$  for each value of  $\lambda$ . As predicted,  $\text{Var}[\partial_{\theta_1} \mathcal{C}]$  exponentially vanishes with the slope of -3.158, -4.103, and -3.965 for the star, ring, and squeezing ansatz, respectively. The star ansatz exhibits slower gradient decay as  $\lambda$  approaches 1 due to its smaller trainable variables' space than the ring and squeezing ansatz. This indicates better training and less susceptibility to vanishing gradients, leading to better achievement of the ultimate quantum bound.

#### E. Multiparameter estimation under the Ornstein-Uhlenbeck model

We consider the Ornstein-Uhlenbeck model, where the noise is induced by the stochastic fluctuation of the external

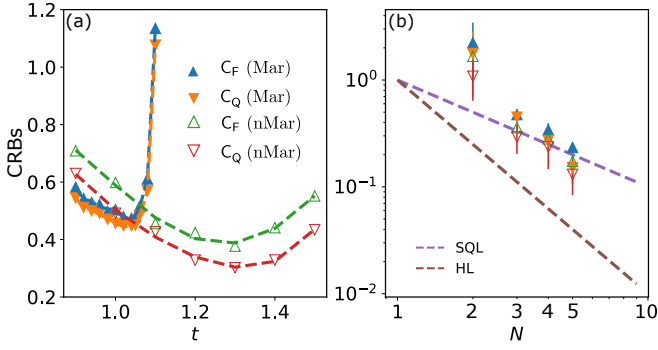


FIG. 5: **Variational quantum metrology under time-dephasing noise.** (a): we present the CRBs as functions of the sensing time, demonstrating an optimal sensing time for achieving each minimum CRB. The non-Markovian dephasing (nMar) produces lower metrological bounds in comparison to the Markovian one (Mar). (b): plot of the minimal bounds for cases in (a), comparing them with the standard quantum limit (SQL) and the Heisenberg limit (HL). For non-Markovian metrology, the bounds surpass the SQL, as predicted.

(magnetic) field [45]. The Kraus operators are [53]

$$K_1(t) = \begin{pmatrix} \sqrt{1-q(t)} & 0 \\ 0 & 1 \end{pmatrix}, K_2(t) = \begin{pmatrix} \sqrt{q(t)} & 0 \\ 0 & 0 \end{pmatrix}, \quad (5)$$

where  $q(t) = 1 - e^{-f(t)}$  with  $f(t) = \gamma[t + \tau_c(e^{-t/\tau_c} - 1)]$ , and  $\tau_c$  represents the memory time of the environment. In the Markovian limit ( $\tau_c \rightarrow 0$ ),  $f(t) = \gamma t$ , which corresponds to the previous dephasing case. In the non-Markovian limit with large  $\tau_c$ , such as  $t/\tau_c \ll 1$ , we have  $f(t) = \frac{\gamma t^2}{2\tau_c}$ . In the numerical simulation, we fixed  $\gamma = 0.1$  and  $\tau_c = 20$  (for non-Markovian)

$$q(t) = \begin{cases} 1 - \exp(-0.1t) & \text{Markovian,} \\ 1 - \exp(-\frac{t^2}{400}) & \text{non-Markovian.} \end{cases} \quad (6)$$

We use this model to study the relationship between sensing time, Markovianity, and ultimate attainability of the quantum bound. Figure 5a displays the optimal CRBs for Markovian and non-Markovian noises as functions of sensing time  $t$ . As previously reported in [18], there exists an optimal sensing time that minimizes the CRBs for each case examined here. Moreover, the non-Markovian dephasing (nMar) provides lower metrological bounds as compared to the Markovian case (Mar). So far, the minimum CRBs for different  $N$  are presented in Figure 5b. The results demonstrate that with an increase in  $N$ , the non-Markovian noise attains a better bound than the standard quantum limit (SQL) for both classical and quantum bounds. This observation is in qualitative agreement with results reported using semidefinite programming [2], indicating the potential of variational optimization for designing optimal non-Markovian metrology experiments. Finally, we note that in the Ornstein-Uhlenbeck model, the quantum bound is unachievable, as indicated by  $C_F > C_Q$ . It remains a question for future research on whether one can attain the quantum bound  $C_Q$  with probe designs, and the possibility for tight bounds in the non-Markovian scenario.

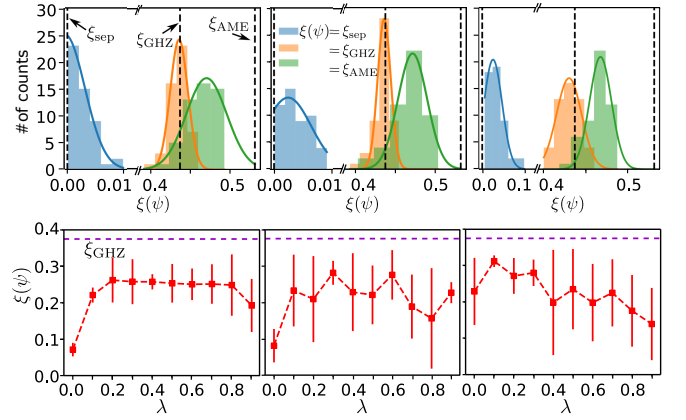


FIG. 6: **Entanglement generation.** (Top): from left to right: the distribution of training CEs corresponds to the star, ring, and squeezing ansatzes, respectively. All the ansatzes can produce separable and GHZ states, but generating an AME state is challenging. The results are shown at  $N = 4$  and (2-2) layers for each ansatz. (Bottom): the CEs are plotted at the optimal CRBs in Fig. 3, using the same circuit setup that in the figure. Again,  $\lambda$  is the dephasing probability.

### III. DISCUSSION

We discuss how the three ansatzes create entangled states and the role of entangled resources in achieving the quantum bound in VQM. We analyze entanglement using the concentratable entanglement (CE) defined by [4]

$$\xi(\psi) = 1 - \frac{1}{2^{|s|}} \sum_{\alpha \in \mathcal{P}(s)} \text{Tr}[\rho_\alpha^2], \quad (7)$$

where  $\mathcal{P}(s)$  is the power set of  $s$ ,  $\forall s \in \{1, 2, \dots, N\}$ , and  $\rho_\alpha$  is the reduced state of  $|\psi\rangle$  in the subsystem  $\alpha$  with  $\rho_\emptyset := \mathbf{I}$ . Practically,  $\xi(\psi)$  can be computed using the SWAP test circuit as stated in Ref. [4], where  $\xi(\psi) = 1 - p(\mathbf{0})$ , with  $p(\mathbf{0})$  is the probability of obtaining  $|00 \dots 0\rangle$ . The ability of the SWAP test to compute CE is due to the equivalence between conditional probability distribution and the definition of CE.

We first train the three ansatzes to evaluate their ability of entangled-state generation. Particularly, the training process aims to generate quantum states with  $\xi(\psi) = \{\xi_{\text{sep}}, \xi_{\text{GHZ}}, \xi_{\text{AME}}\}$ , where  $\xi_{\text{sep}} = 0$  for a separable state,  $\xi_{\text{GHZ}} = \frac{1}{2} - \frac{1}{2^N}$  for a GHZ state, and  $\xi_{\text{AME}} = 1 - \frac{1}{2^N} \sum_{j=0}^N \binom{N}{j} \frac{1}{2^{\min(j, N-j)}}$  for an absolutely maximally entangled (AME) state [8, 11]. The top panels in Fig. 6 display the results for star, ring, and squeezing ansatz, from left to right, at  $N = 4$  and (2-2) layers of each ansatz as an example. All the ansatzes examined can reach the separable and GHZ state, but hard to achieve the AME state. This observation is consistent with the CEs for conventional graph states [8].

We next discuss the role of entanglement in achieving the ultimate quantum bound. In the bottom panels of Fig. 6, we graph the corresponding CEs at the optimal CRBs shown in Fig. 3, which apparently do not require the maximum entanglement (e.g., GHZ) to achieve the ultimate quantum bound. This phenomenon can be explained by the fact that maximum entan-

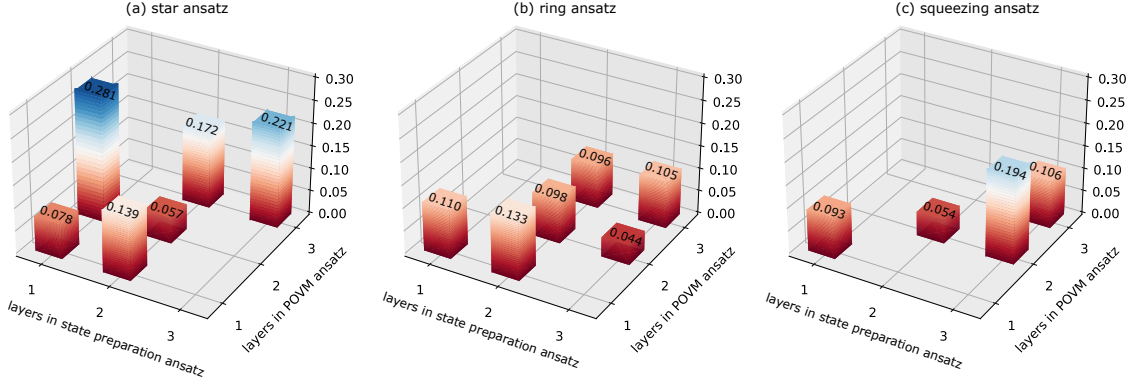


FIG. 7: **Cost function vs the optimal number of layers for different ansatzes.** The plot of the cost function for (a) star ansatz, (b) ring ansatz, and (c) squeezing ansatz at  $N = 3$  without noise. The minimum cost function vs the number of layers are (0.057, 2-2), (0.044, 3-2), and (0.054, 2-2), respectively.

glement is not required for high-precision quantum metrology, as previously noted in Refs. [5, 35, 43]. Therefore, emphasizing the robustness of easily preparable entangled probe states and non-local POVM schemes would be advantageous for quantum metrological applications exposed to Markovian and non-Markovian noises.

#### IV. METHODS

##### A. Quantum circuit training

In numerical simulations, we employ the ADAM optimizer to train the VQM variables [26], where the variables at step  $k + 1$  are given by

$$\theta^{k+1} = \theta^k - \alpha \frac{\hat{m}_k}{\sqrt{\hat{v}_k} + \epsilon}, \quad (8)$$

where  $m_k = \beta_1 m_{k-1} + (1 - \beta_1) \nabla_{\theta} \mathcal{C}(\theta)$ ,  $v_k = \beta_2 v_{k-1} + (1 - \beta_2) \nabla_{\theta}^2 \mathcal{C}(\theta)$ ,  $\hat{m}_k = m_k / (1 - \beta_1^k)$ ,  $\hat{v}_k = v_k / (1 - \beta_2^k)$ , with the hyper-parameters are chosen as  $\alpha = 0.2$ ,  $\beta_1 = 0.8$ ,  $\beta_2 = 0.999$  and  $\epsilon = 10^{-8}$ . The gradient  $\partial_{\theta_i} \mathcal{C}(\theta)$  is given through the parameter-shift rule [33, 40]. The simulations are performed in Qiskit Aer simulator [38]. The number of iterations is chosen using the EarlyStopping callback [24].

To determine the appropriate number of layers for the preparation state and POVM ansatzes, we analyze the cost function (2) with different number of layers. We use  $(\star, \dagger - \ddagger)$  to denote the minimum cost function, the number of layers for

variational state preparation, and the number of layers for variational POVM. The results are shown in Fig. 7 with  $(\star, \dagger - \ddagger) = (0.057, 2-2)$ ,  $(0.04, 3-2)$ , and  $(0.054, 2-2)$  for the star, ring, and squeezing ansatz, respectively. Obviously, the metrological performances of these ansatzes demonstrate that deep ansatzes are unnecessary. For the numerical simulations presented in this paper, we keep the number of layers fixed at these values.

##### B. Computing Fisher information

Classical and quantum Fisher information matrices can be computed in quantum circuits using the finite difference approximation. For the CFIM, we first derive an output probability as  $\partial_{\phi_i} p = \frac{p(\phi_i+s) - p(\phi_i-s)}{2s}$ , for a small shift  $s$ . We then compute the CFIM from  $F_{ij} = \sum_m \frac{1}{p(m|\phi)} [\partial_{\phi_i} p(m|\phi)] [\partial_{\phi_j} p(m|\phi)]$ . For the QFIM, we explicitly derive  $Q_{ij} = 2 \text{vec}[\partial_{\phi_i} \rho(\phi)]^\dagger [\rho(\phi)^* \otimes I + I \otimes \rho(\phi)]^+ \text{vec}[\partial_{\phi_j} \rho(\phi)]$ , where  $\text{vec}[\cdot]$  is the vectorization of a matrix, and the superscript ‘+’ denotes the pseudo-inversion [20]. Again, we apply the finite difference to compute  $\partial_{\phi_i} \rho = \frac{\rho(\phi_i+s) - \rho(\phi_i-s)}{2s}$ , and substitute into the above equations to compute the QFIM.

##### Acknowledgments

We thank C.Q. Nguyen for assisting with the initial code. This work is supported by JSPS KAKENHI Grant Number 23K13025.

- 
- [1] Francesco Albarelli, Jamie F. Friel, and Animesh Datta. Evaluating the holevo cramér-rao bound for multiparameter quantum metrology. *Phys. Rev. Lett.*, 123:200503, Nov 2019.
  - [2] Anian Altherr and Yuxiang Yang. Quantum metrology for non-markovian processes. *Phys. Rev. Lett.*, 127:060501, Aug 2021.
  - [3] O E Barndorff-Nielsen and R D Gill. Fisher information in quantum statistics. *Journal of Physics A: Mathematical and*

- General*, 33(24):4481, jun 2000.
- [4] Jacob L. Beckey, N. Gigena, Patrick J. Coles, and M. Cerezo. Computable and operationally meaningful multipartite entanglement measures. *Phys. Rev. Lett.*, 127:140501, Sep 2021.
- [5] Daniel Braun, Gerardo Adesso, Fabio Benatti, Roberto Floreanini, Ugo Marzolino, Morgan W. Mitchell, and Stefano Pirandola. Quantum-enhanced measurements without entanglement.

- Rev. Mod. Phys.*, 90:035006, Sep 2018.
- [6] Samuel L. Braunstein and Carlton M. Caves. Statistical distance and the geometry of quantum states. *Phys. Rev. Lett.*, 72:3439–3443, May 1994.
  - [7] G. Carrara, M. G. Genoni, S. Cialdi, M. G. A. Paris, and S. Olivares. Squeezing as a resource to counteract phase diffusion in optical phase estimation. *Phys. Rev. A*, 102:062610, Dec 2020.
  - [8] Alice R. Cullen and Pieter Kok. Calculating concentratable entanglement in graph states. *Phys. Rev. A*, 106:042411, Oct 2022.
  - [9] Rafał Demkowicz-Dobrzański, Jan Czajkowski, and Pavel Sekatski. Adaptive quantum metrology under general markovian noise. *Phys. Rev. X*, 7:041009, Oct 2017.
  - [10] Rafał Demkowicz-Dobrzański, Wojciech Górecki, and Mădălin Guță. Multi-parameter estimation beyond quantum fisher information. *Journal of Physics A: Mathematical and Theoretical*, 53(36):363001, aug 2020.
  - [11] M Enríquez, I Wintrowicz, and K Życzkowski. Maximally entangled multipartite states: A brief survey. *Journal of Physics: Conference Series*, 698(1):012003, mar 2016.
  - [12] Jamie Friel, Pantita Palittapongarnpim, Francesco Albarelli, and Animesh Datta. Attainability of the holevo-cramér-rao bound for two-qubit 3d magnetometry, 2020.
  - [13] Akio Fujiwara. Strong consistency and asymptotic efficiency for adaptive quantum estimation problems. *Journal of Physics A: Mathematical and General*, 39(40):12489, sep 2006.
  - [14] Manuel Gessner, Augusto Smerzi, and Luca Pezzè. Multiparameter squeezing for optimal quantum enhancements in sensor networks. *Nature Communications*, 11(1):3817, Jul 2020.
  - [15] Vittorio Giovannetti, Seth Lloyd, and Lorenzo Maccone. Advances in quantum metrology. *Nature Photonics*, 5(4):222–229, Apr 2011.
  - [16] M. Hayashi, editor. *Asymptotic Theory of Quantum Statistical Inference: Selected Papers*. World Scientific Singapore, 2005.
  - [17] C. W. Helstrom. *Quantum Detection and Estimation Theory*. Academic Press, New York, 1976.
  - [18] Le Bin Ho, Hideaki Hakoshima, Yuichiro Matsuzaki, Masayuki Matsuzaki, and Yasushi Kondo. Multiparameter quantum estimation under dephasing noise. *Phys. Rev. A*, 102:022602, Aug 2020.
  - [19] A.S. Holevo. *Probabilistic and Statistical Aspects of Quantum Theory*. Springer, New York, 1st edition, 2011.
  - [20] Dominik Šafránek. Simple expression for the quantum fisher information matrix. *Phys. Rev. A*, 97:042322, Apr 2018.
  - [21] Raphael Kaubruegger, Pietro Silvi, Christian Kokail, Rick van Bijnen, Ana Maria Rey, Jun Ye, Adam M. Kaufman, and Peter Zoller. Variational spin-squeezing algorithms on programmable quantum sensors. *Phys. Rev. Lett.*, 123:260505, Dec 2019.
  - [22] Raphael Kaubruegger, Denis V. Vasilyev, Marius Schulte, Klemens Hammerer, and Peter Zoller. Quantum variational optimization of ramsey interferometry and atomic clocks. *Phys. Rev. X*, 11:041045, Dec 2021.
  - [23] Steven Kay. *Estimation theory, Vol 1*. Prentice Hall, Englewood Cliffs, NJ, 1st edition, 1993.
  - [24] Keras. Earlystopping callback - keras documentation. [https://keras.io/api/callbacks/early\\_stopping/](https://keras.io/api/callbacks/early_stopping/), 2021. [Online; accessed 28-March-2023].
  - [25] E. M. Kessler, I. Lovchinsky, A. O. Sushkov, and M. D. Lukin. Quantum error correction for metrology. *Phys. Rev. Lett.*, 112:150802, Apr 2014.
  - [26] Diederik P Kingma and Jimmy Ba. Adam: A method for stochastic optimization. In *Proceedings of the 3rd International Conference on Learning Representations (ICLR)*, 2015.
  - [27] Bálint Koczor, Suguru Endo, Tyson Jones, Yuichiro Matsuzaki, and Simon C Benjamin. Variational-state quantum metrology. *New Journal of Physics*, 22(8):083038, aug 2020.
  - [28] Bálint Koczor, Suguru Endo, Tyson Jones, Yuichiro Matsuzaki, and Simon C Benjamin. Variational-state quantum metrology. *New Journal of Physics*, 22(8):083038, aug 2020.
  - [29] Ziqi Ma, Pranav Gokhale, Tian-Xing Zheng, Sisi Zhou, Xiaofei Yu, Liang Jiang, Peter Maurer, and Frederic T. Chong. Adaptive circuit learning for quantum metrology. In *2021 IEEE International Conference on Quantum Computing and Engineering (QCE)*, pages 419–430, 2021.
  - [30] Lorenzo Maccone and Alberto Riccardi. Squeezing metrology: a unified framework. *Quantum*, 4:292, July 2020.
  - [31] K Matsumoto. A new approach to the cramér-rao-type bound of the pure-state model. *Journal of Physics A: Mathematical and General*, 35(13):3111, mar 2002.
  - [32] Johannes Jakob Meyer, Johannes Borregaard, and Jens Eisert. A variational toolbox for quantum multi-parameter estimation. *npj Quantum Information*, 7(1):89, Jun 2021.
  - [33] K. Mitarai, M. Negoro, M. Kitagawa, and K. Fujii. Quantum circuit learning. *Phys. Rev. A*, 98:032309, Sep 2018.
  - [34] Klaus Mølmer and Anders Sørensen. Multiparticle entanglement of hot trapped ions. *Phys. Rev. Lett.*, 82:1835–1838, Mar 1999.
  - [35] M. Oszmaniec, R. Augusiak, C. Gogolin, J. Kołodyński, A. Acín, and M. Lewenstein. Random bosonic states for robust quantum metrology. *Phys. Rev. X*, 6:041044, Dec 2016.
  - [36] Shengshi Pang and Andrew N. Jordan. Optimal adaptive control for quantum metrology with time-dependent hamiltonians. *Nature Communications*, 8(1):14695, Mar 2017.
  - [37] Marco G A Paris. Quantum state estimation. *International Journal of Quantum Information*, 7(1):125–137, 2009.
  - [38] Qiskit. Aer provider tutorial, 2021.
  - [39] Sammy Ragy, Marcin Jarzyna, and Rafał Demkowicz-Dobrzański. Compatibility in multiparameter quantum metrology. *Phys. Rev. A*, 94:052108, Nov 2016.
  - [40] Maria Schuld, Ville Bergholm, Christian Gogolin, Josh Izaac, and Nathan Killoran. Evaluating analytic gradients on quantum hardware. *Phys. Rev. A*, 99:032331, Mar 2019.
  - [41] Nathan Shettell and Damian Markham. Graph states as a resource for quantum metrology. *Phys. Rev. Lett.*, 124:110502, Mar 2020.
  - [42] Jasinder S. Sidhu, Yingkai Ouyang, Earl T. Campbell, and Pieter Kok. Tight bounds on the simultaneous estimation of incompatible parameters. *Phys. Rev. X*, 11:011028, Feb 2021.
  - [43] Todd Tilma, Shinichiro Hamaji, W. J. Munro, and Kae Nemoto. Entanglement is not a critical resource for quantum metrology. *Phys. Rev. A*, 81:022108, Feb 2010.
  - [44] Géza Tóth and Iagoba Apellaniz. Quantum metrology from a quantum information science perspective. *Journal of Physics A: Mathematical and Theoretical*, 47(42):424006, oct 2014.
  - [45] G. E. Uhlenbeck and L. S. Ornstein. On the theory of the brownian motion. *Phys. Rev.*, 36:823–841, Sep 1930.
  - [46] Mihai D. Vidrighin, Gaia Donati, Marco G. Genoni, Xian-Min Jin, W. Steven Kolthammer, M. S. Kim, Animesh Datta, Marco Barbieri, and Ian A. Walmsley. Joint estimation of phase and phase diffusion for quantum metrology. *Nature Communications*, 5(1):3532, Apr 2014.
  - [47] Samson Wang, Enrico Fontana, M. Cerezo, Kunal Sharma, Akira Sone, Lukasz Cincio, and Patrick J. Coles. Noise-induced barren plateaus in variational quantum algorithms. *Nature Communications*, 12(1):6961, Nov 2021.
  - [48] Yunkai Wang and Kejie Fang. Continuous-variable graph states for quantum metrology. *Phys. Rev. A*, 102:052601, Nov 2020.
  - [49] Koichi Yamagata, Akio Fujiwara, and Richard D. Gill. Quantum

- local asymptotic normality based on a new quantum likelihood ratio. *The Annals of Statistics*, 41(4):2197 – 2217, 2013.
- [50] Jing Yang, Shengshi Pang, Zekai Chen, Andrew N. Jordan, and Adolfo del Campo. Variational principle for optimal quantum controls in quantum metrology. *Phys. Rev. Lett.*, 128:160505, Apr 2022.
- [51] Xiaodong Yang, Xi Chen, Jun Li, Xinhua Peng, and Raymond Laflamme. Hybrid quantum-classical approach to enhanced quantum metrology. *Scientific Reports*, 11(1):672, Jan 2021.
- [52] Yuxiang Yang, Giulio Chiribella, and Masahito Hayashi. Attaining the ultimate precision limit in quantum state estimation. *Communications in Mathematical Physics*, 368(1):223–293, May 2019.
- [53] Ting Yu and J.H. Eberly. Entanglement evolution in a non-markovian environment. *Optics Communications*, 283(5):676–680, 2010. Quo vadis Quantum Optics?
- [54] Yi-Hao Zhang and Wen Yang. Improving spin-based noise sensing by adaptive measurements. *New Journal of Physics*, 20(9):093011, sep 2018.
- [55] Tian-Xing Zheng, Anran Li, Jude Rosen, Sisi Zhou, Martin Koppenhöfer, Ziqi Ma, Frederic T. Chong, Aashish A. Clerk, Liang Jiang, and Peter C. Maurer. Preparation of metrological states in dipolar-interacting spin systems. *npj Quantum Information*, 8(1):150, Dec 2022.
- [56] Sisi Zhou, Mengzhen Zhang, John Preskill, and Liang Jiang. Achieving the heisenberg limit in quantum metrology using quantum error correction. *Nature Communications*, 9(1):78, Jan 2018.
- [57] Huangjun Zhu. Information complementarity: A new paradigm for decoding quantum incompatibility. *Scientific Reports*, 5(1):14317, Sep 2015.